journal of the mechanical behavior of biomedical materials 154 (2024) 106533

Contents lists available at ScienceDirect

Journal of the Mechanical Behavior of Biomedical Materials

journal homepage: www.elsevier.com/locate/jmbbm

Development of ZTA (80% Al_2O_3/20% ZrO_2) pre-sintered blocks for milling in CAD/CAM systems

Adolfo C.O. Lopes [a], Ernesto B. Benalcázar-Jalkh [a,*], Edmara T.P. Bergamo [a,c,d], Tiago M. B. Campos [a], Laura F. de Carvalho [a], Ricardo Tanaka [a,b], Luis A. Genova [e], Satoshi Yamaguchi [f], Lukasz Witek [c,g,h], Paulo G. Coelho [i,j], Estevam A. Bonfante [a]

[a] Department of Prosthodontics and Periodontology, University of São Paulo - Bauru School of Dentistry, Bauru, SP, Brazil
[b] Tanaka Lab, São Paulo, SP, Brazil
[c] Department of Biomaterials and Biomimetics, New York University College of Dentistry, New York, NY, USA
[d] Department of Prosthodontics, NYU Dentistry, New York, NY, 10010, USA
[e] Nuclear and Energy Research Institute, IPEN, SP, Brazil
[f] Department of Dental Biomaterials, Osaka University Graduate School of Dentistry, Suita, Osaka, Japan
[g] Department of Biomedical Engineering, NYU Tandon School of Engineering, New York University, Brooklyn, NY, USA
[h] Hansjörg Wyss Department of Plastic Surgery, NYU Langone Medical Center, New York, NY, USA
[i] DeWitt Daughtry Family Department of Surgery, Division of Plastic Surgery, Miller School of Medicine, University of Miami, Miami, FL, 33136, USA
[j] Department of Biochemistry and Molecular Biology, Miller School of Medicine, University of Miami, Miami, FL, 33136, USA

ARTICLE INFO

Keywords:
Zirconia
Alumina
Blocks
CAD-CAM
Milling
Aging

ABSTRACT

The present work aims to develop a production method of pre-sintered zirconia-toughened-alumina (ZTA) composite blocks for machining in a computer-aided design and computer-aided manufacturing (CAD-CAM) system. The ZTA composite comprised of 80% Al_2O_3 and 20% ZrO_2 was synthesized, uniaxially and isostatically pressed to generate machinable CAD-CAM blocks. Fourteen green-body blocks were prepared and pre-sintered at 1000 °C. After cooling and holder gluing, a stereolithography (STL) file was designed and uploaded to manufacture disk-shaped specimens projected to comply with ISO 6872:2015. Seventy specimens were produced through machining of the blocks, samples were sintered at 1600 °C and two-sided polished. Half of the samples were subjected to accelerated autoclave hydrothermal aging (20h at 134 °C and 2.2 bar). Immediate and aged samples were characterized by scanning electron microscopy (SEM) and X-ray diffraction (XRD). Optical and mechanical properties were assessed by reflectance tests and by biaxial flexural strength test, Vickers indentation and fracture toughness, respectively. Samples produced by machining presented high density and smooth surfaces at SEM evaluation with few microstructural defects. XRD evaluation depicted characteristic peaks of alpha alumina and tetragonal zirconia and autoclave aging had no effect on the crystalline spectra of the composite. Optical and mechanical evaluations demonstrated a high masking ability for the composite and a characteristic strength of 464 MPa and Weibull modulus of 17, with no significant alterations after aging. The milled composite exhibited a hardness of 17.61 GPa and fracture toughness of 5.63 MPa $m^{1/2}$, which remained unaltered after aging. The synthesis of ZTA blocks for CAD-CAM was successful and allowed for the milling of disk-shaped specimens using the grinding method of the CAD-CAM system. ZTA composite properties were unaffected by hydrothermal autoclave aging and present a promising alternative for the manufacture of infrastructures of fixed dental prostheses.

1. Introduction

Although zirconia prostheses have been broadly used in dentistry during the last two decades, the implementation of strong, esthetic, and sufficiently stable materials for long-span fixed dental prostheses (FDPs) has not been completely achieved(Benalcazar-Jalkh et al., 2023).

* Corresponding author. Dept. of Prosthodontics and Periodontology, University of Sao Paulo – Bauru School of Dentistry, Al. Octávio Pinheiro Brisolla 9-75, Bauru, SP, Brazil.
E-mail address: ernestobenalcazarj@gmail.com (E.B. Benalcázar-Jalkh).

https://doi.org/10.1016/j.jmbbm.2024.106533
Received 23 February 2024; Received in revised form 29 March 2024; Accepted 29 March 2024
Available online 1 April 2024

Among dental zirconias, 3 mol% yttria-stabilized tetragonal zirconia polycrystals (3Y-TZP) presents the highest mechanical properties for long span FDPs (Zhang and Lawn, 2018), however, strong clinical evidence has shown that the clinical performance of porcelain veneered 3Y-TZP for teeth- or implant-supported partial and full-arch FDPs present inferior survival rates compared to metal ceramics (Pjetursson et al., 2017; Sailer et al., 2018; Pjetursson et al., 2022). Moreover, the increased incidence of porcelain and framework fractures documented in clinical research has resulted in the consensus that fully veneered zirconia should not be regarded as the primary material choice for (FDPs) (Sailer et al., 2018).

Developments in polycrystalline ceramics have led to the achievement of zirconias with improved translucency indicated for full-contour esthetic reconstructions(Zhang and Lawn, 2017). Changes in composition, processing methods, and an increase in yttrium oxide and cubic phase content have been demonstrated to be effective strategies to enhance the material's translucency, which has resulted in a wide range of zirconia materials, each characterized by unique compositions, properties, and clinical applications(Guth et al., 2019; Zhang et al., 2019). However, concerns related to the hydrothermal stability of monolithic 3Y-TZP (Chevalier et al., 1999; Chevalier, 2006, Piconi et al., 2006; Chevalier et al., 2007) and the trade-off between optical and mechanical properties resulting from the increased cubic content in 4Y- and 5Y-PSZ, remain an issue (Zhao et al., 2017; Zhang et al., 2019).

In light of the limitations inherent to the different zirconias in dentistry, alumina-zirconia composites have emerged as an alternative for metallic and 3Y-TZP infrastructures for long-span FDPs (Bergamo et al., 2020). Zirconia toughened alumina (ZTA), a ceramic composite comprised by an alumina (Al_2O_3) matrix reinforced with the addition of a secondary 3Y-TZP phase(Kurtz et al., 2014) has been extensively used in orthopedics to overcome the detrimental effects of low temperature degradation of 3Y-TZP systems(Chevalier et al., 2000; Chevalier et al., 2009b). The synergistic integration of the advantageous properties of both materials enables the attainment of high mechanical properties, attributed to the transformation toughening effect of 3Y-TZP, as well as the mitigation of low-temperature degradation in zirconia. This is facilitated by the Al_2O_3 hard matrix, which restricts the interconnectivity of zirconia grains(Chevalier and Gremillard, 2009).

In-vitro studies performed with artificial accelerated aging have demonstrated that ZTA composites containing 70–85% Al_2O_3 and 15–30% 3Y-TZP exhibit significant hydrothermal stability. Throughout the aging process, their microstructure, crystalline composition, optical characteristics, and mechanical properties remained unchanged, resembling those observed in 3Y-TZP systems (Benalcazar Jalkh et al., 2020). Particularly, the combination of 80% Al_2O_3 and 20% 3Y-TZP has been presented as a viable option from mechanical and optical perspectives for the manufacture of infrastructures for single crowns and FDPs (Lopes et al., 2020), according to ceramic systems standard requirements (ISO 6872:2015).

However, the evaluations of ZTA composites have been performed *in-vitro* using disk-shaped specimens obtained from uniaxial and/or isostatic pressing, which does not represent entirely the fabrication process currently utilized by computer-aided design and computer-aided manufacturing (CAD-CAM) equipments in dentistry. The primary technique for processing polycrystalline ceramic currently involves machining of green or pre-sintered blocks followed by final sintering to achieve full density and the desired optical and mechanical properties(Yousry et al., 2023). To the best of the authors knowledge, the conformation of ZTA blocks for milling dental restorations has not been previously reported in scientific literature. Therefore, the present study aimed to innovate in the development of a production method for pre-sintered Zirconia-toughened-Alumina composite blocks suitable for milling in CAD-CAM systems. Additionally, the microstructure, optical and mechanical properties of the ZTA milled samples were evaluated before and after autoclave hydrothermal aging. We hypothesized that the synthesized ZTA blocks would be suitable for milling and that the resulting samples would maintain their optical and mechanical properties after aging.

2. Materials and methods

2.1. Ceramic powders and samples preparation

In the present study, ceramic powders of translucent 3Y-TZP (Zpex, Tosoh Corporation, Tokyo, Japan/particle size = 40 nm) and alumina (Baikalox Regular CR10, Baikowski SAS, Annecy, France/particle size = 350 nm) were used as raw materials. Composition of the ceramic powders used in the present study is summarized in Table 1.

For the synthesis of the ZTA composite ceramic powder, a suspension in ethanol containing alumina and zirconia powders (Al_2O_3-80% v.s. ZrO_2-20%) was prepared. The blend was homogenized for 4 h in a friction mill with alumina spheres, the slurry produced was then dried (rotary evaporator 801, Fisaton, São Paulo, Brazil), and the powder was granulated and sieved.

The experimental ZTA powder was then uniaxially pressed at 70.000 psi for 30 s in a steel matrix with dimensions of 15.5 × 19 × 40 mm to prepare green blocks with the desired dimensions. A total of fourteen green-body blocks were prepared, vacuum packed and isostatically pressed at room temperature at 30000 psi for 30 s (Isostatic Press, National Forge, Pensilvania, EUA).

After the conformation of green-body ZTA blocks, a pilot test was performed to determine an optimal pre-sintering protocol to allow for milling. Three additional ZTA blocks were pre-sintered at 900, 1000 and 1100 °C, respectively, and used for the pilot milling test. ZTA blocks pre-sintered at 900 °C presented a porous appearance and fractured frequently during milling. Pre-sintering at 1100 °C resulted in a denser block with a non-uniform milling in the CAD-CAM equipment. Finally, ZTA blocks pre-sintered at 1000 °C allowed for a smooth milling process for the manufacture of disk-shaped ZTA specimens.

Therefore, ZTA blocks were pre-sintered for 1 h in an electric furnace (LHT 04/18 Nabertherm, Bahnhofstr Lilienthal, Germany) at 1000°C with heating and cooling rate of 4° per minute. Pre-sintered ZTA blocks were then glued to specific holders for a CAD-CAM system (Cerec in Lab, Sirona) (Fig. 1A) and mounted to prepare disc-shaped specimens by subtractive manufacturing. For this purpose, an STL file was designed (Fig. 1B) and uploaded to manufacture disk-shaped specimens projected to complain with ISO 6872:2015 for dental ceramics testing.

From the fourteen synthesized green-body blocks, seventy specimens were produced utilizing the "grinding" method of the CAD-CAM system (Cerec in Lab, Sirona). Diamond Step bur 20 and Cylinder pointed bur 20 (left and right side of the milling equipment, respectively) were used to obtain disk-shaped samples as presented in Fig. 2A. Samples were then sintered at 1600 °C for 1 h with a heating and cooling rate of 4 per minute (Electric furnace LHT 04/18 Nabertherm). Polishing was performed in both disk surfaces using a semi-automatic polishing machine (Automet, 2000; Buehler, Illinois, USA) with diamond disks and diamond suspensions of granulations up to 1 μm (ALLIED High-Tech Products, California, USA) (Fig. 2B).

Seventy disc-shaped specimens were prepared with final dimensions of 12-mm of diameter and 1-mm thickness as recommended by the ISO 6872:2015. Density, crystalline structure and surface imaging, as well as optical and mechanical properties were evaluated in the milled samples before and after autoclave accelerated artificial aging. Additionally, fractographic analysis of the fragments was performed.

2.2. Aging

Half of the samples were subject to *in-vitro* low-temperature degradation (LTD) in autoclave (Vitale Class CD, Cristófoli, Campo Mourão, PR, Brasil) at 134 °C, under a 2.2 bar pressure, over a period of 20 h. This protocol has been proven to effectively promote t-m phase transformation in 3Y-TZP-based materials, with a significant impact on its

Table 1
Composition of the ceramic powders used to synthesize the zirconia toughened alumina composite. 3Y-TZP: 3 mol% yttria-stabilized tetragonal zirconia polycrystals.

3Y-TZP Zpex (Tosoh Corporation)	Particle Size (nm)	Chemical Composition [wt.-%]						
		Y_2O_3	Al_2O_3	Na_2O	SiO_2	FeO_2O_3	CaO	MgO
	40	5.2 ± 0.2	≤0.1	≤0.04	≤0.02	≤0.01		
Al_2O_3								
Baikalox Regular CR10 (Baikowski)	Particle Size (nm)	Crystal Structure		Chemical Analyses ICP (ppm)				
		Alpha	Gamma	Fe	Na	Si	Ca	K	Mg, Ti, Cr, Mn, Ni, Cu, Zn
	350	95%	5%	6	13	18	2	22	<1 each

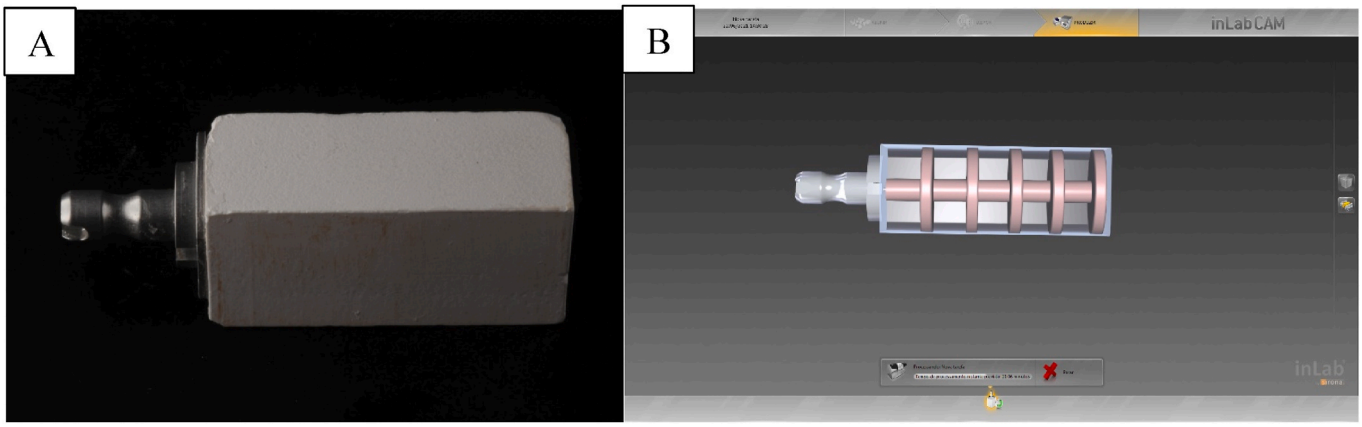

Fig. 1. A) Block after presinterization at 1000 °C, with the adapter for machining in the computer-aided design and computer-aided manufacturing (CAD-CAM) system. B) Interface of the inLab CAM program, showing the optimization of the stereolithography design so that the maximum number of discs can be machined in a single block.

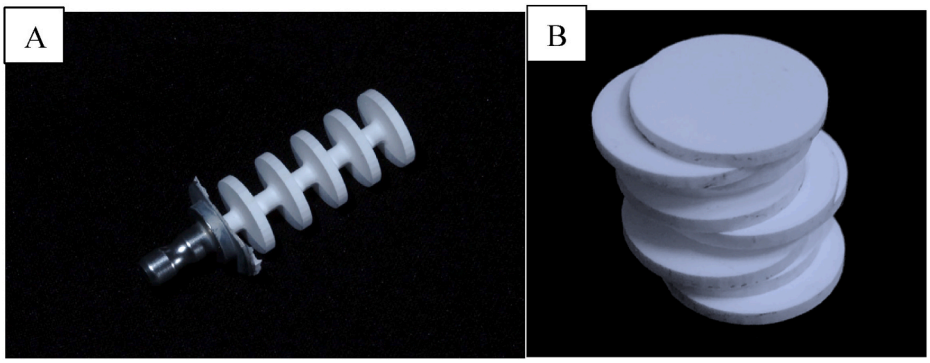

Fig. 2. A) Zirconia toughened alumina (ZTA) block after machining in computer-aided design and computer-aided manufacturing and B) Milled ZTA disk-shaped specimens after polishing.

microstructure and overall properties (Pereira et al., 2015).

2.3. Scanning electron microscope (SEM)

Representative specimens were analyzed by SEM (FEG-SEM, MIRA3-TESCAN, Brno-Kohoutovice, Czech Republic) to visualize the surface characteristics and microstructure of the ZTA ceramic system. SEM images were obtained at high vacuum, 5 kV accelerating voltage, 6–12 mm working distance, and magnifications up to 20k × .

2.4. X-ray diffraction (XRD)

The crystalline structure of ZTA milled samples was analyzed by XRD (X'pert Power PANalytical, Netherlands) before and after aging. The scanning was performed on the Bragg θ-2θ geometry, equipped with a graphite monochromator and Cu Kα radiation (λ = 1.5406 Å), operating at a voltage of 40 kV and a current emission of 40 mA. The data were obtained in periods of 1.0 s and steps of 0.020 (2θ) of 20–70°. Baseline subtraction was performed in HighScore Plus Software (Malvern Panalytical Ltd, Westborough, Massachusetts, USA) for all XRD collected data. Based on the obtained data, a Rietveld analysis was conducted to quantify the crystalline phases found in the experimental material (Arata et al., 2014).

2.5. Optical properties evaluation

The optical properties of the ZTA composite were analyzed in a spectrophotometer (CM 26 dG, Konica Minolta, Tokyo, Japan) that operates in the wavelengths range of visible light (400–700 nm) (n = 10/group). Contrast ratio (CR) and translucency parameter (TP) were

calculated by means of reflectance test values obtained on white (Yw) and black (Yb) backgrounds.

CR is the property that measures the transparency or opacity of the material and is measured by the ratio of reflectance of the specimen on the black background (Yb) to the reflectance of the same specimen on a white background (Yw), which is given by: $CR = Yb/Yw$.

TP, which represents the masking ability of the material, was obtained by the color difference calculation (ΔE_{00}) of the specimens over black and white backgrounds, according to the CIEDE2000 equation:

$$\Delta E_{00} = \left[\left(\frac{\Delta L'}{K_L S_L}\right)^2 + \left(\frac{\Delta C'}{K_C S_C}\right)^2 + \left(\frac{\Delta H'}{K_H S_H}\right)^2 + R_T\left(\frac{\Delta C'}{K_C S_C}\right)\left(\frac{\Delta H'}{K_H S_H}\right)\right]^{1/2}$$

Where $\Delta L'$, $\Delta C'$, and $\Delta H'$ represent the differences in lightness, chroma and hue between specimens. R_T is a function that accounts for the interaction between chroma and hue differences in the blue region. S_L, S_C, and S_H are the weighting functions and K_L, K_C, and K_H are the correction terms to be adjusted in accordance with the experimental conditions (Sharma et al., 2005; Paravina et al., 2015; Volpato et al., 2016).

2.6. Vickers Hardness and fracture toughness

Hardness and fracture toughness were determined by the Vickers indentation method using microhardness testing equipment (DuraScan, Emco-test, Kuchl, Austria). In each sample, ten indentations were measured under a load of 3 kg and dwell time of 30 s. Vickers microhardness values were calculated by:

$$HV = 0.1891L/d^2$$

where, L is the load (N) and d is the arithmetic mean of the length of the two diagonals (mm).

Fracture toughness (K_{IC}) was calculated according to the following equation (Arcila et al., 2021, de Sousa Lima, Gall et al., 2022):

$$K_{IC} = 0.035\left(\frac{l}{a}\right)^{\frac{-1}{2}}\left(\frac{H_v}{E\Phi}\right)^{\frac{-2}{5}}\left(\frac{H_v\, a^{\frac{1}{2}}}{\Phi}\right)$$

where K_{IC} is the fracture toughness (MPa·m$^{1/2}$); "l" is the length of the crack measured from the tip of the indentation to the tip of the crack (μm); "a" is half length of the indentation diagonal (μm); "HV" is Vickers hardness (GPa); "E" is Young's modulus (GPa) and "Φ" is the dimensionless constant developed by Niihara (Φ = 2.7) (Niihara, 1983).

2.7. Biaxial flexural strength (BFS) test

BFS test of thirty samples per group was performed using a piston-on-three balls device, as per ISO 6872:2015 recommendations. An all-electric equipment (ElectroPulsTM E3000 Linear-Torsion, Instron, Norwood, MA) was used at a crosshead speed of 0.5 mm/min until failure. The maximum load was recorded for each specimen, and the BFS was calculated using the following equations:

$$\sigma = -0.2387P(X - Y)/b^2$$

$$X = (1+\nu)ln\,(r_2/r_3)^2 + [(1-\nu)/2](r_2/r_3)^2$$

$$Y = (1+\nu)\left[1 + ln\,(r_1/r_3)^2\right] + (1-\nu)(r_1/r_3)^2$$

where, σ is BFS (MPa), P the fractured load (N), b is the specimen thickness at fracture site (1.2 ± 0.2 mm), v is the Poisson's ratio (0.25), r_1 the radius of support circle (5.5 mm), r_2 the radius of loaded area (0.75 mm), and r_3 is the radius of the specimen (6 mm).

The probability of survival as a function of Characteristic strength was calculated to stresses of 100, 300, and 500 MPa, which are the ISO 6872:2015 required strength for single unit, 3-unit anterior substructures (up to premolar), and 3-unit posterior substructures for FDPs, respectively.

2.8. Statistical analysis

Data from optical properties, Vickers hardness and fracture toughness were tabulated and subjected to descriptive analysis, normality, and homoscedasticity test. Data normality and homoscedasticity were confirmed using Shapiro-Wilk ($p > 0.05$) and Levene ($p > 0.25$) tests. Repeated-measures analyses of variance and Tukey tests were used for statistical evaluation of differences with an overall significance level of 5% using SPSS software (IBM SPSS Statistics version 27, Armonk, NY). Data are presented as a function of the estimated mean and 95% confidence interval (CI). Biaxial flexural strength data were analyzed using Weibull 2-parameter distribution (Weibull ++22, Reliasoft, Tucson, AZ, USA). Weibull parameters [Characteristic stress (MPa) and Weibull modulus (*m*)] were calculated, and a contour plot was graphed to determine differences between groups. The probability of survival as function of characteristic stress were calculated to stresses of 100, 300, and 500 MPa.

3. Results

The processing method used for manufacturing ZTA blocks was successful, and the pre-sintered blocks obtained were suitable for milling geometric samples. SEM surface evaluation of the ZTA composite block depicted morphological characteristics of a dense crystalline matrix with a homogeneous distribution of 3Y-TZP grains, as observed in different magnifications in Fig. 3.

Further SEM evaluation comprised the qualitative analysis of the ZTA disks milled from the blocks. The micrographs depicted the achievement of a dense polycrystalline surface in the composite with the presence of few microstructural defects related to the ceramic processing. Remarkably, the density evaluation of unpolished fully sintered samples through Archimedes method revealed a final density of 98% for the composite. After accelerated hydrothermal aging in autoclave, no significant changes were observed at the microstructural analysis through SEM images, as presented in Fig. 4.

The XRD spectra of the milled ZTA disks before and after artificial aging are presented in Fig. 5. Typical peaks of alpha (α) alumina and tetragonal (t) zirconia can be identified in the spectra obtained from the non-aged samples. Slight transformation was observed after aging, with characteristic monoclinic (m) peaks depicted in the spectra. Quantification of the tetragonal-to-monoclinic (t-m) phase transformation through Rietveld analysis demonstrated a 15.9% of monoclinic phase after the aging protocol. Considering that there is only 20% zirconia in the matrix, this equates to 3.17% of phase transformation.

Results of optical properties evaluations are summarized in Table 2. Overall, a high masking ability and low translucency was observed for the ZTA composite with no significant differences in contrast ratio and translucency parameter before and after aging ($p = 0.662$ and 0.781, respectively).

The Vickers hardness fracture toughness results are also presented in Table 2. ZTA samples manufactured by milling demonstrated Vickers hardness of 17 GPa with no statistical difference after aging ($p = 0.777$). Likewise, fracture toughness evaluation through the indentation method depicted no significant differences in milled ZTA before and after aging (5.63 and 5.26 MPa m$^{1/2}$, respectively) ($p = 0.730$).

The characteristic strength and Weibull modulus for the milled ZTA samples are presented in Table 3. The Weibull modulus of ZTA samples presented no significant differences after hydrothermal aging, where values ranging from 15.9 to 17.12 were observed before and after aging, respectively. Failure distribution for ceramic samples is typically assessed by the Weibull modulus, a shape parameter of the Weibull distribution, which describes the variation in strength values as a result

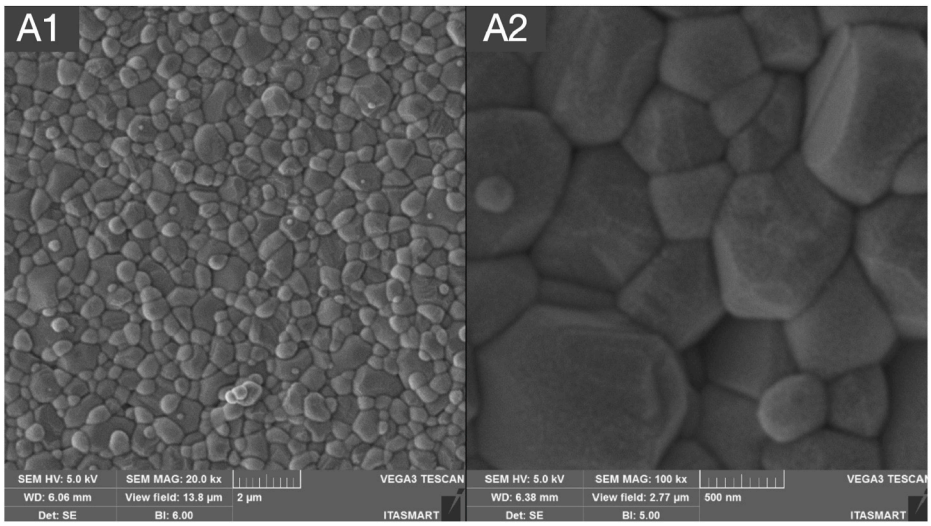

Fig. 3. Scanning electron microscopic images of zirconia toughened alumina composite block surface with A) 20k X and B) 100k × magnifications. The images demonstrate the microstructural arrangement obtained for the experimental fabrication of the computer-aided design and computer-aided manufacturing blocks.

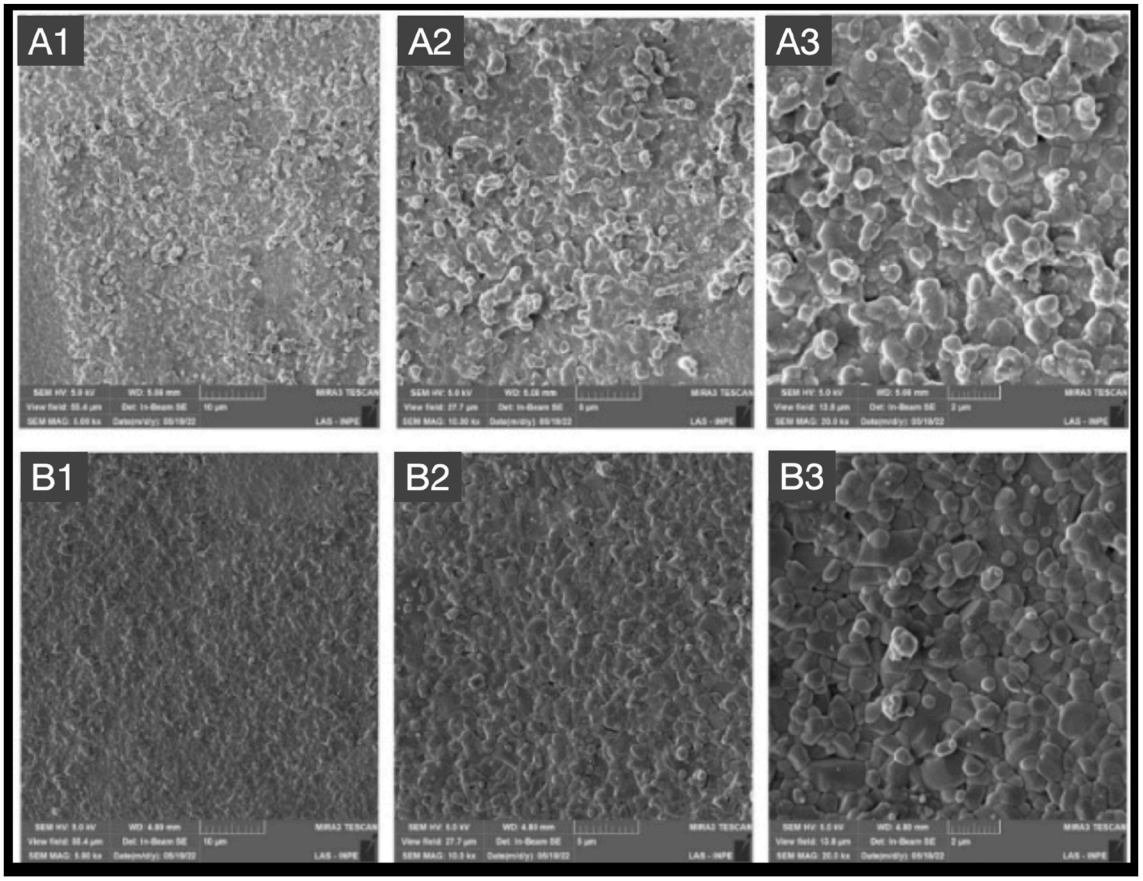

Fig. 4. Scanning electron microscopic images of milled zirconia toughned alumina samples before (A) and after (B) accelerated hydrothermal aging in autoclave with 5k (1), 10k (2) and 20k × (3) magnifications.

of defects population in the material structure. Furthermore, the characteristic strength of milled ZTA samples, which describes the strength at which 62.3% would fail, ranged from 457 to 464 MPa for the immediate and aged conditions, with no significant differences after hydrothermal aging. The use level probability Weibull plot presented in the Fig. 6A shows the reliability distribution of samples as a function of characteristic strength. Furthermore, the relation between Weibull parameters is didactically presented in a Contour plot (Fig. 6B) where the absence of overlaps between contours denotes the absence of statistically significant differences among groups.

Table 4 presents the survival probability results for a given mission at 100, 300, and 500 MPa, which correspond to indications for single crowns, 3-unit fixed partial dentures in the anterior region, and 3-unit fixed partial dentures in the posterior region, respectively, according

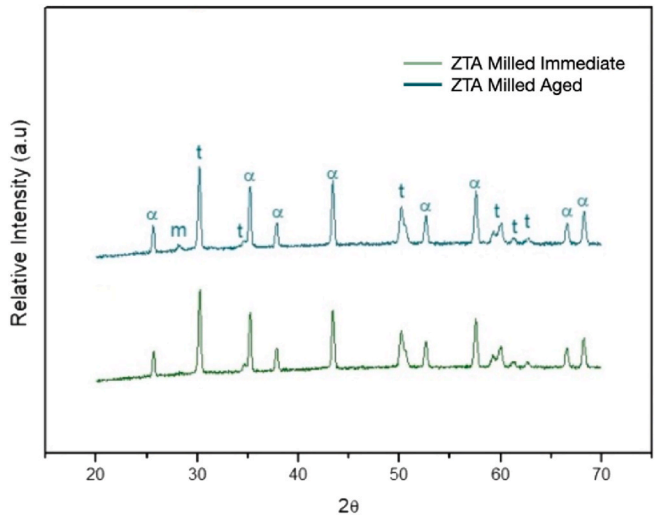

Fig. 5. X-ray diffraction (XRD) patterns of the milled experimental zirconia toughened alumina composite before and after aging. Characteristic alpha (α) alumina, tetragonal (t) and monoclinic (m) zirconia peaks are depicted in the XRD spectra with a slight increase of monoclinic phase after aging.

Table 2
Summary of the results of optical properties (Contrast Ratio and Translucency Parameter), Vickers Hardness and Fracture Toughness evaluation of milled zirconia toughened alumina (ZTA) samples before and after aging. Data is presented as mean values with correspondent 95% confidence intervals.

Milled ZTA	Contrast Ratio	Translucency Parameter	Vickers Hardness (GPa)	Fracture Toughness ($MPa \bullet m^{1/2}$)
Immediate	1.00 (0.005) A	1.41 (0.12) A	17.61 (0.75) A	5.63 (0.52) A
Aged	0.99 (0.005) A	1.45 (0.12) A	17.18 (0.75) A	5.26 (0.65) A

Similar letters denote absence of significant differences among conditions.

Table 3
Weibull modulus and Characteristic strength (MPa) and their respective 95% confidence bounds for the milled zirconia toughened alumina (ZTA) composite before and after hydrothermal autoclave aging.

Milled ZTA	Immediate	Aged
Upper Bound	21.1	21.3
Weibull Modulus	**17.12 a**	**15.9 a**
Lower Bound	13.8	11.9
Upper Bound	473	468
Characteristic strength	**464 a**	**457 a**
Lower Bound	455	446

Similar letters indicate absence of statistically significant difference between conditions.

to ISO 6872:2015.

For missions at 100 and 300 MPa, the ZTA composite presented high survival probability (>99%). However, for missions at 500 MPa, a significant reduction in reliability (2%) was observed for immediate and aged groups. Aging did not affect the reliability of the ZTA composite for any of the given missions.

4. Discussion

The results of the present study demonstrated the success of the synthesis and processing method for manufacturing experimental ZTA blocks. The milled ZTA discs presented a dense microstructure with spherical and homogeneous grains, and a typical crystalline content of alpha alumina and tetragonal zirconia. Milled samples also exhibited high opacity and masking ability, and mechanical properties compatible with the indication for fixed prostheses of up to 3 units in the anterior region (ISO 6872:2015). Furthermore, all characterizations and properties remained unchanged after the hydrothermal aging process, indicating high stability of the developed ZTA system after milling. Therefore, the hypothesis of the present study was accepted.

The primary technique for producing infrastructures of polycrystalline ceramic systems is still the milling of pre-sintered blocks in CAD-CAM systems. After milling, the infrastructure is sintered to achieve final density, and the desired optical and mechanical properties (Yousry et al., 2023). Although some studies have investigated the properties and clinical performance of 3Y-TZP infrastructures (Kelly, 1999, Guazzato et al., 2004), there is still a lack of information regarding the feasibility of processing pre-sintered ZTA blocks. In the present study, after the conformation of ZTA blocks, a pilot test was performed to determine the pre-sintering protocol to achieve optimal properties to allow for milling. Pre-sintering temperatures of 900, 1000 and 1100 °C were used to produce ZTA blocks for the pilot milling test. While ZTA blocks pre-sintered at 900 °C presented a porous appearance and consistently fractured during milling, pre-sintering at 1100 °C produced a denser block and a non-uniform milling procedure in the CAD-CAM equipment. Thus, pre-sintering at 1000 °C was used for the study where a smooth milling process was observed and allowed for the manufacture of disk-shaped ZTA specimens. The use of the grinding method on method of the CAD-CAM system equipped with diamond burs (Step bur 20 and Cylinder pointed bur 20) were paramount to achieve a smooth process without compromise of the pre-sintered block. Therefore, the proposed method for milling ZTA blocks was successful and resulted in a density of 98% according to the Archimedes' principle. These results are consistent with data presented by ZTA composites in previous studies (Benalcazar Jalkh et al., 2020; Bergamo et al., 2020; Lopes et al., 2020).

The *in-vitro* simulation of hydrothermal degradation using autoclave has been demonstrated to effectively induce zirconia t-m phase transformation (Pereira et al., 2015) and is recognized as a standard method according to ISO 13356:2015.(International-Standard-Organization, 2015). While ISO protocol (autoclave aging at 134°C, 2.2 bar, for 5 h) has been correlated in orthopedic literature to be equivalent to 2–4 years *in-vivo* aging, (Chevalier et al., 1999) caution has been advised in the extrapolation of *in-vitro* results to *in-vivo* scenarios. Clinical evidence suggest that aging can occur up to three times faster than conventionally accepted *in vitro-in vivo* extrapolations(Kocjan et al., 2020). Therefore, an extensive hydrothermal aging protocol in autoclave was applied in the present study following the recommendations of previous literature (Pereira et al., 2015). It is noteworthy that the milled ZTA samples presented a similar aging behavior as the same material processed by uniaxial pressing of discs in previous studies(Lopes et al., 2020). Although a small percentage of transformation was observed in ZTA samples after aging (~3%), monoclinic phase was significantly lower than that reported for 3Y-TZP systems after aging (~28.25%). The same artificial aging protocol has also been used in previous studies investigating the low temperature degradation susceptibility of ZTA composites comprised by different proportions of zirconia within the alumina matrix (15–30%), which demonstrated similar aging behavior as the one observed in the present study (Casellas et al., 1999; Benalcázar Jalkh, Bergamo et al., 2020; Benalcazar Jalkh, Monteiro et al., 2020; Lopes et al., 2020).

Regarding the optical properties results, the ZTA composite presented high opacity and masking ability before and after hydrothermal aging. This behavior fosters its indication as infrastructure material for FDPs on darkened substrates and over metal components, with subsequent porcelain veneering to achieve esthetics. While the contrast ratio values obtained for the milled ZTA composite were similar to those reported for the ZTA samples manufactured by uniaxial pressing (CR: 0.99), higher translucency parameter values were observed for milled

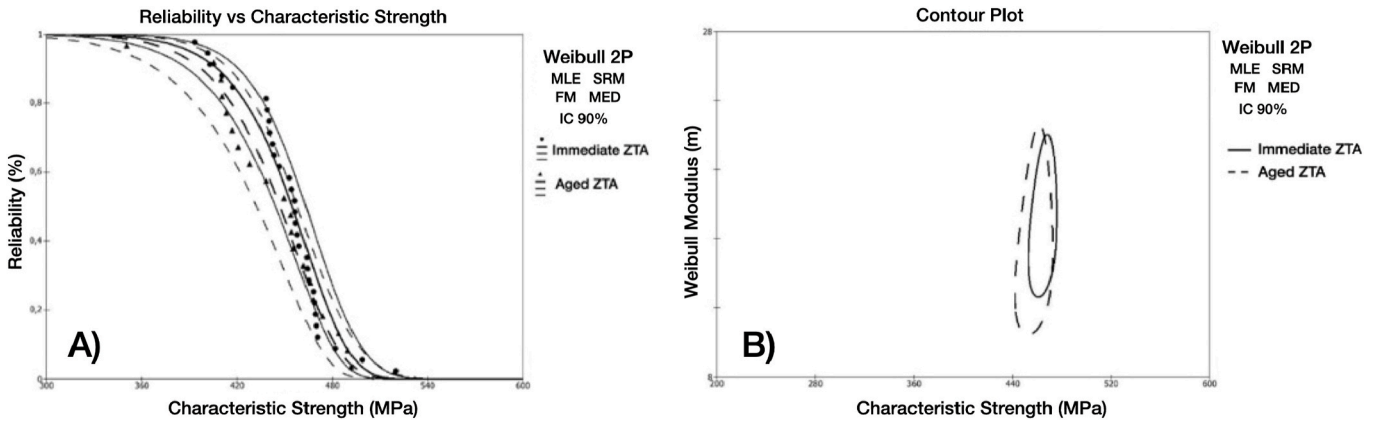

Fig. 6. A) Use level probability Weibull curves show sample reliability distribution as a function of characteristic strength. B) Contour plot of Characteristic strength (MPa) versus. Weibull modulus (*m*) of milled zirconia toughened alumina (ZTA). The overlap of contours denotes statistical homogeneity.

Table 4
Probability of survival with corresponding 95% confidence bounds. ZTA: zirconia toughened alumina.

Milled ZTA	Immediate	Aged
Upper Bound	100	100
100 MPa	**100 aA**	**100 aA**
Lowe Bound	100	100
Upper Bound	99	99
300 MPa	**99 aB**	**99 aB**
Lowe Bound	99	98
Upper Bound	8	7
500 MPa	**2 aC**	**1.5 aC**
Lowe Bound	0	0

Different lowercase letters indicate statistical difference between aging conditions. Different uppercase letters indicate statistical difference between missions.

samples (TP: 1.41) regarding samples manufactured by pressing (TP: 0.18) (Lopes et al., 2020). This fact may be associated with the pre-sintering stage of ZTA blocks at 1000 °C for 1 h before milling. This temperature serves as a nucleation point for ZTA, potentially resulting in a higher number of nuclei with a more uniform distribution of zirconia grains and grain size. Additionally, it may lead to a lower defect population, which directly influences the optical properties of the system (Becher and Swain, 1992, de Araujo-Junior et al., 2020).

The extensive hydrothermal aging protocol used in the present study did not alter the Vickers hardness (~17 GPa) and fracture toughness (~5.5 MPa $m^{1/2}$) of the milled ZTA. Moreover, the failure data obtained in the BFS test indicate that the ZTA composite's Weibull modulus (~15) and Characteristic strength (~450 MPa) were not affected by hydrothermal aging. Previous literature that evaluated the mechanical properties of polycrystalline composites suggests that ZTA composites with 15%, 20%, and 30% ZrO_2 present fracture toughness values of 6, 7, and 9 MPa $m^{1/2}$, respectively, where the increase in mechanical properties is influenced by the concentration of 3Y-TZP in the composite (Casellas et al., 2003). These values are comparable to those reported for Vickers Hardness and fracture toughness of pure 3Y-TZP systems (900-1300 MPa and 6–9 MPa $m^{1/2}$, respectively) (Guess et al., 2011, Tang et al., 2012; Anusavice and C. Rawls, 2013; Sequeira et al., 2016).

The characteristic strength of milled ZTA was significantly lower than the values previously reported for uniaxially pressing of the same material (20% Zr_2O - 80% Al_2O_3) (σ: ~800 MPa). Furthermore, the milled ZTA presented the lowest characteristic strength when compared with uniaxially pressed ZTA disks comprised by different zirconia-alumina concentrations (σ15%: ~950 MPa; σ30%: ~915 MPa) (Benalcázar Jalkh et al., 2020; Benalcazar Jalkh et al., 2020a; Lopes et al., 2020). Such result may be associated with the number of steps and defects induced during the processing of ceramic discs by milling compared to the direct pressing of the specimen. The stability of the ZTA composite before and after aging was consistent with data from previous studies and represents a significant advantage for the clinical applicability of this system in the long term. In fact, the effects of low-temperature degradation have been extensively documented for 3Y-TZP systems, where significant alterations in strength have been reported after hydrothermal aging(Chevalier et al., 2007; Chevalier et al., 2009a; Pereira et al., 2015; Borges et al., 2019). Data from recently published clinical studies raise concerns regarding the long-term stability of rehabilitations based on 3Y-TZP systems, where the effects of low-temperature degradation have been observed in monolithic prostheses after six months with a continue progression after two years, propagating from the surface to a depth of tens of micrometers (Koenig et al., 2021; Koenig et al., 2023).

Despite the reduction in characteristic strength values, milled ZTA samples meet the strength prerequisites for indication as partially or fully covered infrastructure for fixed prostheses of up to three units in the anterior region, with a survival probability over 90% for a mission at 300 MPa (ISO 6872:2015). These findings encourage further studies to increase flexural strength of the ZTA composite and to determine better parameters for the processing of ZTA blocks and milling due to their potential use in the dental field. Moreover, several limitations must be acknowledged for the present in-vitro study, including the absence of pure Alumina and 3Y-TZP control groups, the absence of milling of anatomical samples, and the evaluation of mechanical properties through single load to failure tests, which do not represent the cycling loading and damage accumulation that occur during oral function. Therefore, testing these materials for fatigue performance is paramount to characterize their lifetime. Moreover, in-vitro to in-vivo extrapolations of aging behavior should be made with caution considering the significant differences in aging kinetics reported in clinical and laboratorial investigations (Kocjan et al., 2020; Koenig et al., 2021; Koenig et al., 2023). Thus, clinical studies are required to evaluate the performance of ZTA-based prosthesis.

5. Conclusion

The synthesize and milling of ZTA composite blocks in a CAD-CAM system was successful and the milled samples presented high resistance to hydrothermal aging. The composite presented high reliability for missions at 100 and 300 MPa (99%), consistent with the indication as infrastructure of FDPs of up to three units in the anterior region. Further developments are required for its indication for higher load applications.

CRediT authorship contribution statement

Adolfo C.O. Lopes: Writing – original draft, Software, Methodology, Investigation, Formal analysis, Conceptualization. **Ernesto B. Benalcázar-Jalkh:** Writing – review & editing, Writing – original draft, Validation, Software, Investigation, Conceptualization. **Edmara T.P. Bergamo:** Writing – original draft, Validation, Methodology, Formal analysis, Data curation, Conceptualization. **Tiago M.B. Campos:** Writing – original draft, Visualization, Validation, Methodology, Investigation, Formal analysis. **Laura F. de Carvalho:** Visualization, Validation, Methodology, Investigation, Data curation. **Ricardo Tanaka:** Validation, Supervision, Resources, Methodology, Investigation, Data curation. **Luis A. Genova:** Visualization, Validation, Supervision, Methodology, Data curation, Conceptualization. **Satoshi Yamaguchi:** Writing – review & editing, Visualization, Validation, Supervision, Software, Data curation. **Lukasz Witek:** Writing – review & editing, Visualization, Validation, Supervision, Investigation, Data curation. **Paulo G. Coelho:** Writing – review & editing, Validation, Supervision, Resources, Funding acquisition, Conceptualization. **Estevam A. Bonfante:** Writing – review & editing, Validation, Supervision, Software, Resources, Project administration, Funding acquisition, Formal analysis, Conceptualization.

Declaration of competing interest

The authors declare that they have no known competing financial interests or personal relationships that could have appeared to influence the work reported in this paper.

Data availability

Data will be made available on request.

Acknowledgments:

This work was supported by São Paulo Research Foundation (FAPESP), grants 2012/19078-7,2021/06730-7, EMU 2022/05496-3 and 2022/05495-7; and scholarships # 2019/14798-0, 2022/07157-1, 2019/08693-1, 2021/08018-2, 2020/12874-9. By Conselho Nacional de Desenvolvimento Científico e Tecnológico (CNPq), Grant # 307255/2021-2. By CAPES Financial Code 001.

References

Anusavice, K.S., C. Rawls, H.R., 2013. Phillips' Science of Dental Materials. Elsevier Inc.
Arata, A., Campos, T.M., Machado, J.P., Lazar, D.R., Ussui, V., Lima, N.B., Tango, R.N., 2014. Quantitative phase analysis from X-ray diffraction in Y-TZP dental ceramics: a critical evaluation. J. Dent. 42 (11), 1487–1494.
Arcila, L.V.C., de Carvalho Ramos, N., Campos, T.M.B., Dapieve, K.S., Valandro, L.F., de Melo, R.M., Bottino, M.A., 2021. Mechanical behavior and microstructural characterization of different zirconia polycrystals in different thicknesses. J. Advan. Prosthodontics 13 (6), 385.
Becher, P.F., Swain, M.V., 1992. Grain-size-dependent transformation behavior in polycrystalline tetragonal zirconia. J. Am. Ceram. Soc. 75 (3), 493–502.
Benalcázar Jalkh, E.B., Bergamo, E.T.P., Monteiro, K.N., Cesar, P.F., Genova, L.A., Lopes, A.C.O., Lisboa Filho, P.N., Coelho, P.G., Santos, C.F., Bortolin, F., Piza, M.M. T., Bonfante, E.A., 2020. Aging resistance of an experimental zirconia-toughened alumina composite for large span dental prostheses: optical and mechanical characterization. J. Mech. Behav. Biomed. Mater. 104, 103659.
Benalcazar Jalkh, E.B., Monteiro, K.N., Cesar, P.F., Genova, L.A., Bergamo, E.T.P., Lopes, A.C.O., Lima, E., Lisboa-Filho, P.N., Campos, T.M.B., Witek, L., Coelho, P.G., Borges, A.F.S., Bonfante, E.A., 2020a. Aging resistant ZTA composite for dental applications: microstructural, optical and mechanical characterization. Dent. Mater. 36 (9), 1190–1200.
Benalcazar Jalkh, E.B., Monteiro, K.N., Cesar, P.F., Genova, L.A., Bergamo, E.T.P., Lopes, A.C.O., Lima, E., Lisboa-Filho, P.N., Campos, T.M.B., Witek, L., Coelho, P.G., Borges, A.F.S., Bonfante, E.A., 2020b. Aging resistant ZTA composite for dental applications: microstructural, optical and mechanical characterization. Dent. Mater.
Benalcazar-Jalkh, E.B., Bergamo, E.T.P., Campos, T.M.B., Coelho, P.G., Sailer, I., Yamaguchi, S., Alves, L.M.M., Witek, L., Tebcherani, S.M., Bonfante, E.A., 2023. A narrative review on polycrystalline ceramics for dental applications and proposed update of a classification system. Materials 16 (24).
Bergamo, E.T.P., Cardoso, K.B., Lino, L.F.O., Campos, T.M.B., Monteiro, K.N., Cesar, P.F., Genova, L.A., Thim, G.P., Coelho, P.G., Bonfante, E.A., 2020. Alumina-toughened zirconia for dental applications: physicochemical, mechanical, optical, and residual stress characterization after artificial aging. J. Biomed. Mater. Res. B Appl. Biomater.
Borges, M.A.P., Alves, M.R., dos Santos, H.E.S., dos Anjos, M.J., Elias, C.N., 2019. Oral degradation of Y-TZP ceramics. Ceram. Int. 45 (8), 9955–9961.
Casellas, D., Nagl, M.M., Llanes, L., Anglada, A., 2003. Fracture toughness of alumina and ZTA ceramics: microstructural coarsening effects. J. Mater. Process. Technol. 143, 148–152.
Casellas, D., Rafols, I., Llanes, L., Anglada, M., 1999. Fracture toughness of zirconia–alumina composites. Int. J. Refract. Metals Hard Mater. 17 (1), 11–20.
Chevalier, J., 2006. What future for zirconia as a biomaterial? Biomaterials 27 (4), 535–543.
Chevalier, J., Cales, B., Drouin, J.M., 1999. Low-temperature aging of Y-TZP ceramics. J. Am. Ceram. Soc. 82 (8), 2150–2154.
Chevalier, J., De Aza, A.H., Fantozzi, G., Schehl, M., Torrecillas, R., 2000. Extending the lifetime of ceramic orthopaedic implants. Adv. Mater. 12 (21), 1619–1621.
Chevalier, J., Grandjean, S., Kuntz, M., Pezzotti, G., 2009a. On the kinetics and impact of tetragonal to monoclinic transformation in an alumina/zirconia composite for arthroplasty applications. Biomaterials 30 (29), 5279–5282.
Chevalier, J., Gremillard, L., 2009. Ceramics for medical applications: a picture for the next 20 years. J. Eur. Ceram. Soc. 29 (7), 1245–1255.
Chevalier, J., Gremillard, L., Deville, S., 2007. Low-temperature degradation of Zirconia and implications for biomedical implants. Annu. Rev. Mater. Res. 37, 1–32.
Chevalier, J., Gremillard, L., Virkar, A.V., Clarke, D.R., 2009b. The tetragonal-monoclinic transformation in zirconia: lessons learned and future trends. J. Am. Ceram. Soc. 92 (9), 1901–1920.
de Araujo-Junior, E.N.S., Bergamo, E.T.P., Campos, T.M.B., Benalcazar Jalkh, E.B., Lopes, A.C.O., Monteiro, K.N., Cesar, P.F., Tognolo, F.C., Tanaka, R., Bonfante, E.A., 2020. Hydrothermal degradation methods affect the properties and phase transformation depth of translucent zirconia. J. Mech. Behav. Biomed. Mater. 112, 104021.
de Sousa Lima, E., Gall, C.C., Alves, M.F.R., de Campos, J.B., Campos, T.M.B., dos Santos, C., 2022. Development and characterization of alumina-toughened zirconia (ATZ) ceramic composites doped with a beneficiated rare-earth oxide extracted from natural ore. J. Mater. Res. Technol. 16, 451–460.
Guazzato, M., Proos, K., Quach, L., Swain, M.V., 2004. Strength, reliability and mode of fracture of bilayered porcelain/zirconia (Y-TZP) dental ceramics. Biomaterials 25 (20), 5045–5052.
Guess, P.C., Schultheis, S., Bonfante, E.A., Coelho, P.G., Ferencz, J.L., Silva, N.R., 2011. All-ceramic systems: laboratory and clinical performance. Dent. Clin. 55 (2), 333–352 ix.
Guth, J.F., Stawarczyk, B., Edelhoff, D., Liebermann, A., 2019. Zirconia and its novel compositions: what do clinicians need to know? Quintessence Int. 50 (7), 512–520.
International-Standard-Organization, 2015. ISO 13356:2015 Implants for Surgery — Ceramic Materials Based on Yttria-Stabilized Tetragonal Zirconia (Y-TZP).
Kelly, J.R., 1999. Clinically relevant approach to failure testing of all-ceramic restorations. J. Prosthet. Dent 81 (6), 652–661.
Kocjan, A., Cotic, J., Kosmac, T., Jevnikar, P., 2020. In vivo aging of zirconia dental ceramics - Part I: biomedical grade 3Y-TZP. Dent. Mater.
Koenig, V., Bekaert, S., Dupont, N., Vanheusden, A., Le Goff, S., Douillard, T., Chevalier, J., Djaker, N., Lamy de la Chapelle, M., Amiard, F., Dardenne, N., Wulfman, C., Mainjot, A., 2021. Intraoral low-temperature degradation of monolithic zirconia dental prostheses: results of a prospective clinical study with ex vivo monitoring. Dent. Mater. 37 (7), 1134–1149.
Koenig, V., Douillard, T., Chevalier, J., Amiard, F., Lamy de la Chapelle, M., Le Goff, S., Vanheusden, A., Dardenne, N., Wulfman, C., Mainjot, A., 2023. Intraoral low-temperature degradation of monolithic zirconia dental prostheses: 5-year results of a prospective clinical study with ex vivo monitoring. Dent. Mater.
Kurtz, S.M., Kocagoz, S., Arnholt, C., Huet, R., Ueno, M., Walter, W.L., 2014. Advances in zirconia toughened alumina biomaterials for total joint replacement. J. Mech. Behav. Biomed. Mater. 31, 107–116.
Lopes, A.C.O., Coelho, P.G., Witek, L., Benalcázar Jalkh, E.B., Gênova, L.A., Monteiro, K. N., Cesar, P.F., Lisboa-Filho, P.N., Bergamo, E.T.P., Ramalho, I.S., Campos, T.M.B., Bonfante, E.A., 2020. Microstructural, mechanical, and optical characterization of an experimental aging-resistant zirconia-toughened alumina (ZTA) composite. Dent. Mater. 36 (12), e365–e374.
Niihara, K., 1983. A fracture mechanics analysis of indentation-induced Palmqvist crack in ceramics. J. Mater. Sci. Lett. 2 (5), 221–223.
Paravina, R.D., Ghinea, R., Herrera, L.J., Bona, A.D., Igiel, C., Linninger, M., Sakai, M., Takahashi, H., Tashkandi, E., Mar Perez, M.d., 2015. Color difference thresholds in dentistry. J. Esthetic Restor. Dent. 27, S1–S9.
Pereira, G.K.R., Venturini, A.B., Silvestri, T., Dapieve, K.S., Montagner, A.F., Soares, F.Z. M., Valandro, L.F., 2015. Low-temperature degradation of Y-TZP ceramics: a systematic review and meta-analysis. J. Mech. Behav. Biomed. Mater. 55, 151–163.
Piconi, C., Maccauro, G., Pilloni, L., Burger, W., Muratori, F., Richter, H.G., 2006. On the fracture of a zirconia ball head. J. Mater. Sci. Mater. Med. 17 (3), 289–300.
Pjetursson, B.E., Fehmer, V., Sailer, I., 2022. EAO position paper: material selection for implant-supported restorations. Int. J. Prosthodont. (IJP) 35 (1), 7–16.
Pjetursson, B.E., Sailer, I., Makarov, N.A., Zwahlen, M., Thoma, D.S., 2017. Corrigendum to "All-ceramic or metal-ceramic tooth-supported fixed dental prostheses (FDPs)? A systematic review of the survival and complication rates. Part II: multiple-unit FDPs" [Dental Materials 31 (6) (2015) 624-639]. Dent. Mater. 33 (1), e48–e51.
Sailer, I., Strasding, M., Valente, N.A., Zwahlen, M., Liu, S., Pjetursson, B.E., 2018. A systematic review of the survival and complication rates of zirconia-ceramic and

metal-ceramic multiple-unit fixed dental prostheses. Clin. Oral Implants Res. 29 (Suppl. 16), 184–198.
Sequeira, S., Fernandes, M.H., Neves, N., Almeida, M.M., 2016. Development and characterization of zirconia-alumina composites for orthopedic implants. Ceram. Int. 43 (1), 693–703.
Sharma, G., Wu, W., Dalal, E.N., 2005. The CIEDE2000 color-difference formula: implementation notes, supplementary test data, and mathematical observations. In: Color Research & Application: Endorsed by Inter-Society Color Council, the Colour Group (Great Britain), Canadian Society for Color, Color Science Association of Japan, Dutch Society for the Study of Color, the Swedish Colour Centre Foundation, Colour Society of Australia, vol. 30. Centre Français de la Couleur, pp. 21–30, 1.
Tang, D., Lim, H.B., Lee, K.J., Lee, C.H., Cho, W.S., 2012. Evaluation of mechanical reliability of zirconia-toughened alumina composites for dental implants. Ceram. Int. 38, 2429–2436.
Volpato, C.Â.M., Cesar, P.F., Bottıno, M.A., 2016. Influence of accelerated aging on the color stability of dental zirconia. J. Esthetic Restor. Dent. 28 (5), 304–312.
Yousry, M.A., Hammad, I.A., El Halawani, M.T., Aboushelib, M.N., 2023. Effect of sintering time on microstructure and optical properties of yttria-partially stabilized monolithic zirconia. Dent. Mater. 39 (12), 1169–1179.
Zhang, F., Reveron, H., Spies, B.C., Van Meerbeek, B., Chevalier, J., 2019. Trade-off between fracture resistance and translucency of zirconia and lithium-disilicate glass ceramics for monolithic restorations. Acta Biomater. 91, 24–34.
Zhang, Y., Lawn, B.R., 2017. Novel zirconia materials in dentistry. J. Dent. Res. 22034517737483.
Zhang, Y., Lawn, B.R., 2018. Novel zirconia materials in dentistry. J. Dent. Res. 97 (2), 140–147.
Zhao, M., Sun, Y., Zhang, J., Zhang, Y., 2017. Novel translucent and strong submicron alumina ceramics for dental restorations. J. Dent. Res. 22034517733742.